

Review

The History Goes On: Century Long Study of Romano's Star [†]

Olga Maryeva ^{1,2,*} , Roberto F. Viotti ³, Gloria Koenigsberger ⁴ , Massimo Calabresi ⁵, Corinne Rossi ⁶ and Roberto Gualandi ⁷

¹ Astronomical Institute of the Czech Academy of Sciences, Fričova 298, 25165 Ondřejov, Czech Republic

² Sternberg Astronomical Institute, Lomonosov Moscow State University, Universitetsky pr. 13, 119234 Moscow, Russia

³ INAF-Istituto di Astrofisica e Planetologia Spaziali di Roma (IAPS-INAf), Via del Fosso del Cavaliere 100, 00133 Roma, Italy; roberto.viotti@iaps.inaf.it

⁴ Instituto de Ciencias Físicas, Universidad Nacional Autónoma de México, Ave. Universidad S/N, 62210 Cuernavaca, Mexico; gloria@astro.unam.mx

⁵ Associazione Romana Astrofili, Via Carlo Emanuele I, n°12A, 00185 Roma, Italy; m.calabresi@mclink.it

⁶ Physics Department, Università di Roma "La Sapienza", Piazza le Aldo Moro 5, 00185 Roma, Italy; corinne.rossi@uniroma1.it

⁷ INAF-Osservatorio Astronomico di Bologna, Via Ranzani 1, I-40127 Bologna, Italy; roberto.gualandi@inaf.it

* Correspondence: olga.maryeva@gmail.com

[†] Based on observations made with the Gran Telescopio Canarias (GTC), installed at the Spanish Observatorio del Roque de los Muchachos of the Instituto de Astrofisica de Canarias, in the island of La Palma, and with the Cassini 1.52-m telescope of the Bologna Observatory (Italy), as well as data retrieved from the public archive of the Special Astrophysical observatory of Russian Academy of Sciences (SAO RAS).

Received: 31 July 2019; Accepted: 13 September 2019; Published: 18 September 2019



Abstract: GR 290 (M 33 V0532 = Romano's Star) is a unique variable star in the M33 galaxy, which simultaneously displays variability typical for luminous blue variable (LBV) stars and physical parameters typical for nitrogen-rich Wolf-Rayet (WR) stars (WN). As of now, GR 290 is the first object which is confidently classified as a post-LBV star. In this paper, we outline the main results achieved from extensive photometric and spectroscopic observations of the star: the structure and chemical composition of its wind and its evolution over time, the systematic increase of the bolometric luminosity during the light maxima, the circumstellar environment. These results show that the current state of Romano's Star constitutes a fundamental link in the evolutionary path of very massive stars.

Keywords: galaxies: individual (M 33); stars: individual (GR 290, M 33 V0532); stars: variables: S Doradus; stars: Wolf-Rayet; stars: evolution; stars: winds, outflows

1. Introduction

GR 290 (M 33 V0532 = Romano's Star)¹ is a variable star in M 33 galaxy discovered by Giuliano Romano [1] who originally constructed its light curve and classified it as a Hubble-Sandage variable based on its photometric properties. Later, in 1984, Peter Conti [2] introduced a new class of objects which assimilated Hubble-Sandage variables—luminous blue variables (LBV), and thus GR 290 became an LBV candidate [3,4]. This classification has later been supported by the spectroscopic [5] and

¹ The object has coordinates $\alpha = 01 : 35 : 09.701$, $\delta = +30 : 41 : 57.17$ at J2000 epoch.

photometric [6] studies, as well as by its large bolometric luminosity [7]. However, some arguments suggest that the object is rather on a post-LBV stage already [8–10].

Romano's star displays both strong spectral and photometric variability, with several significant (about 1.5–2 mag) increases of brightness detected during its long monitoring (Polcaro et al. [10] and references therein). Such variability is typical for LBV stars, while in the Hertzsprung-Russell (H-R) GR 290 lies in Wolf-Rayet (WR) stars region, beyond LBV instability strip [10]. GR 290 is presently in a short, and thus very rare, transition phase between the LBV evolutionary phase and the nitrogen rich WR stellar class (WN). It is an extremely important target for studies of massive star evolution, especially the evolutionary link between LBVs, WR stars and supernovae (SNe).

In this paper we summarise the main results achieved in the study of Romano's star. We combine new studies of GR 290's vicinity (Section 2) with its updated century-long photometric light curve (Section 3). Then, based on spectral data, numerical simulations of its stellar atmosphere (Section 4) and the nebula surrounding it (Section 5), we discuss the current evolutionary stage of the star in Section 6.

2. Stellar Vicinity of Romano's Star

GR 290 is located in the outer spiral arm of the M 33 galaxy, and lies to the east of the OB 88 and OB 89 associations [11–13], located at 0.5 and 0.125 kpc projected distances², respectively. The most detailed information about photometry of stars in this area may be found in Massey et al. [15]. Figure 1 shows the identification chart of the object and its vicinity, with red symbols corresponding to the stars which were spectrally classified by Massey et al. [16]. Coordinates and spectral classes of the stars are listed in Table 1.

Massey and Johnson [17] found a couple of carbon-rich Wolf-Rayet (WC) stars in these associations, J013458.89+304129.0 (WC4) in OB 88 and J013505.37+304114.9 (WC4-5) in OB 89. Moreover, the OB 88 association contains the star J013500.30+304150.9 classified as an LBV candidate by Massey et al. [18], and later reclassified by Humphreys et al. [9] as a FeII emission-line star. The presence of evolved massive stars in the associations indicates that their age is close to that of GR 290 and that they might have a common origin. Therefore, it is quite reasonable to suppose that GR 290 might have been originally ejected from the OB 89 association. Then, assuming a median escape velocity for runaway stars of 40–200 km/s [19], this ejection would have to have occurred 3.0–0.6 Myr ago, which is consistent with the evolutionary age of GR 290 and with the age of the OB 89 association.

² The adopted distance to M 33 is 847 ± 61 kpc (distance module 24.64 ± 0.15) from Galletti et al. [14].

Table 1. Stars in the vicinity of GR290 spectrally classified by Massey et al. [16] (and references therein). Names and coordinates are given according to Massey et al. [15]. The three stars also included in Table 2 are marked by boldface.

Name	Coordinates		Spectral Class	V [mag]	(B – V)
	α	δ			
J013449.49+304127.2	01:34:49.46	+30:41:27.1	YSG:	16.468	0.854
J013453.20+304242.8	01:34:53.17	+30:42:42.7	G/KV	17.031	0.906
J013453.97+304043.4	01:34:53.94	+30:40:43.3	RSG:	19.492	1.558
J013454.31+304109.8	01:34:54.28	+30:41:09.7	RSG	18.450	2.045
J013455.06+304114.4	01:34:55.03	+30:41:14.3	B0I+Neb	18.246	−0.103
J013457.20+304146.1	01:34:57.17	+30:41:46.0	B3I	18.872	−0.088
J013458.77+304151.7	01:34:58.74	+30:41:51.6	RSG	19.121	1.605
J013458.89+304129.0	01:34:58.86	+30:41:28.9	WC4	20.662	0.238
J013459.07+304154.9	01:34:59.04	+30:41:54.8	RSG	19.030	1.986
J013459.08+304142.8	01:34:59.05	+30:41:42.7	B2I:	19.306	−0.163
J013459.29+304128.0	01:34:59.26	+30:41:27.9	B0.5:I	18.822	−0.112
J013459.39+304201.2	01:34:59.36	+30:42:01.1	O8Iaf ^a	18.254	−0.142
J013459.81+304156.9	01:34:59.78	+30:41:56.8	RSG:	19.156	1.531
J013500.30+304150.9	01:35:00.27	+30:41:50.8	cLBV ^b	19.298	−0.073
J013500.32+304147.3	01:35:00.29	+30:41:47.2	B0-2I	20.995	−0.183
J013501.36+304149.6	01:35:01.33	+30:41:49.5	Late O/Early B	19.346	−0.279
J013501.71+304159.2	01:35:01.68	+30:41:59.1	B1.5Ia	18.076	−0.099
J013502.06+304034.2	01:35:02.03	+30:40:34.1	RSG	18.500	1.365
J013502.30+304153.7	01:35:02.27	+30:41:53.6	B0.5Ia	18.933	−0.099
J013505.37+304114.9	01:35:05.34	+30:41:14.8	WC4-5	19.061	−0.293
J013505.74+304101.9	01:35:05.71	+30:41:01.8	O6III(f)+Neb	18.218	−0.207
J013506.87+304149.8	01:35:06.84	+30:41:49.7	B0.5Ib	18.655	−0.181
J013507.43+304132.6	01:35:07.40	+30:41:32.5	RSG	18.582	1.991
J013507.53+304208.4	01:35:07.50	+30:42:08.3	RSG	19.961	1.739

^a later classified as Of/late-WN by Humphreys et al. [20]; ^b later classified as a FeII emission-line star by Humphreys et al. [9].

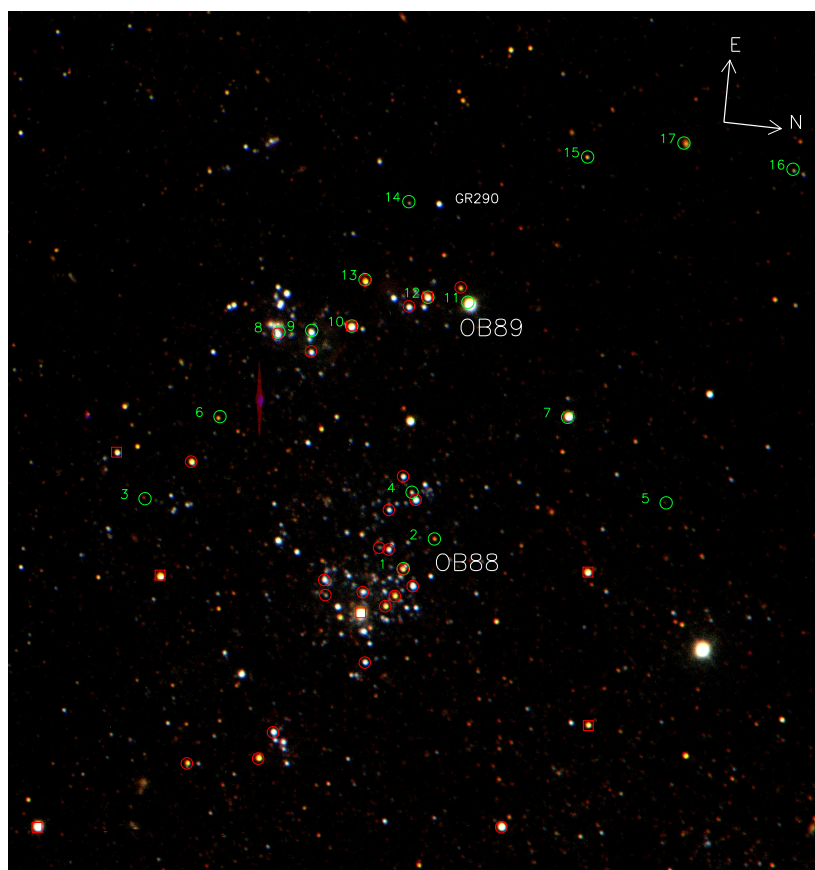


Figure 1. Identification chart of GR 290 vicinity and OB 88 and OB 89 associations. The colour picture is a combination of three direct images, with blue corresponding to B filter, green—to V and red—to R filter, all obtained with 2.5 m telescope of the Caucasian Mountain Observatory (CMO) of the Sternberg Astronomical Institute of Moscow State University. Green circles mark the stars studied in this work and red ones studied by Massey et al. [15,16]. Red squares are stars considered to be foreground objects by Massey et al. [15].

The field around GR 290 is not yet sufficiently explored as it consists mostly of faint ($V > 18$ mag) stars that require large telescopes for acquiring the spectra. Fortunately, some of the surrounding stars happened to lay on the slit during the long-slit observations of the object, thus that analysis of such data may provide additional information on the stellar contents and interstellar extinction in the vicinity of Romano's star. Therefore, we retrieved from General observational archive of Special Astrophysical observatory of Russian Academy of Sciences (SAO RAS)³ all long-slit spectra of GR 290 obtained on Russian 6-m telescope with the Spectral Camera with Optical Reducer for Photometric and Interferometric Observations (SCORPIO) [21] during the years 2005–2016. We also utilised the spectra obtained with the OSIRIS spectrograph on the *Gran Telescopio Canarias* (GTC) and analysed by Maryeva et al. [22] and Maryeva et al. [23]. We reduced these spectra in a uniform way using the ScoRE package⁴ initially created for the SCORPIO data reduction, and extracted the spectra of all stars crossed by the slit. To perform the spectral classification of these stars, we used an automatic code based on the χ^2 fitting with spectral standards from STELIB⁵ (see Le Borgne et al. [24]) in the same way as used by Maryeva et al. [25]. The stars with spectra extracted and analysed in this way are

³ General observational archive of Special Astrophysical observatory is available at <https://www.sao.ru/oasis/cgi-bin/fetch?lang=en>.

⁴ ScoRE package available at <http://www.sao.ru/hq/ssl/maryeva/score.htm>.

⁵ STELIB is available at <http://webast.ast.obs-mip.fr/stelib>.

marked with green circles in Figure 1, and their estimated spectral classes, measured positions and photometric magnitudes are listed in Table 2. The resulting spectra of the stars in flux units are shown in Figures A1–A5.

Table 2. The sample of stars in the field around GR 290 studied in this work. N corresponds to the labels in Figure 1. V and $(B - V)$ taken from Massey et al. [15].

N	Coordinates		Spectral Class	V	$(B - V)$	Instrument
	α	δ		[mag]		
1 ^a	01:34:59.79	+30:41:56.9	RSG / M0-M1	19.156	1.531	OSIRIS
2	01:35:00.69	+30:42:07.5	RSG / K3-K4	20.507	1.613	OSIRIS
3	01:35:00.90	+30:40:18.2	RSG / K5-M0			SCORPIO
4	01:35:01.87	+30:41:57.3	B5-B7	19.980	−0.079	OSIRIS
5	01:35:02.37	+30:43:32.1	F:	21.773	0.059	OSIRIS
6	01:35:03.29	+30:40:42.5	RSG / K-M	20.339	1.088	SCORPIO
7	01:35:04.37	+30:42:53.1	G4-K1	16.459	0.733	SCORPIO
8 ^b	01:35:05.76	+30:41:02.2	star with em.lines			SCORPIO
9	01:35:05.87	+30:41:14.2	star with em.lines	18.522	−0.082	SCORPIO
10 ^c	01:35:06.14	+30:41:29.0	F4-F6 V	17.365	0.561	SCORPIO
11	01:35:07.09	+30:42:12.4	F4-F7 V	14.888	0.592	SCORPIO
12 ^d	01:35:07.15	+30:41:56.3	G8-K1	17.793	0.962	OSIRIS
13 ^e	01:35:07.40	+30:41:32.5	RSG / M0-M1	18.582	1.991	SCORPIO
14	01:35:09.63	+30:41:46.1	A9-F0	20.817	0.246	OSIRIS SCORPIO
15	01:35:11.40	+30:42:50.8	F4-G2 V	20.164	0.647	SCORPIO
16	01:35:11.66	+30:44:08.3	hot star	20.490	0.161	SCORPIO
17	01:35:12.05	+30:43:27.2	cool star	20.149	1.220	SCORPIO
	01:35:14.10	+30:44:23.3	hot star with abs.lines	17.654	−0.038	SCORPIO

^{a,e} Stars classified as RSG by Massey et al. [16]; ^b star classified as O6III(f)+Neb by Massey et al. [16]; ^{c,d} stars classified as foreground objects by Massey et al. [15].

As we can see in Figure 1, our sample of stars partially intersect with the ones studied by Massey et al. [15,16]. We were able to refine the estimates of spectral classes for J013459.81+304156.9 and J013507.43+304132.6, classified earlier as just red supergiants (RSG) [16], as well as for J013506.17+304129.1 and J013507.18+304156.4 as foreground objects according to Massey et al. [15]. Our sample contains three more RSGs, which were not previously reported, and four hot stars, with only one (J013505.74+304101.9 with O6III(f)+Neb spectral class) known before [16]. Among three others, the spectrum of J013505.76+304102.21 displays the He I emission and strong nebular lines. The second one, J013514.1+304423.21, has a spectral slope corresponding to high temperature, and shows H and He absorption lines, while the last, J013501.87+304157.3, was preliminary classified as B5–B7 supergiant.

Knowing the spectral classes of these stars, and therefore their intrinsic colour indices, allows us to estimate the interstellar extinction around GR 290. Its value is comparable to the galactic foreground extinction value of $E_{(B-V)} = 0.052$ (according to the NED extinction calculator [26]). We did not register any star with higher reddening in the vicinity of GR 290.

3. Photometry

Photometric observations of GR 290 were initiated in the early 1960s by the Italian astronomer Giuliano Romano in the Asiago Observatory [1]. He obtained a light curve with the brightness of a star varying irregularly between 16^m.7 and 18^m.1, and classified it as a variable of the Hubble-Sandage type based on the shape of the light curve and GR 290's colour index.

Subsequent photometric investigations of GR 290 were undertaken by Kurtev et al. [6] and later by Zharova et al. [27]. The cumulative light curve derived in the latter work and covering half a century shows that GR 290 exhibits irregular light variations with different amplitudes and time scales [27]. The star shows large and intricate wave-like variations, with duration of the waves amounting to several years. In general, its variability is irregular, with the power spectrum fairly approximated by

a red power-law spectrum [28] (i.e., the one dominated by a long timescale variations). Moreover, Kurtev et al. [6] discovered short-timescale variability with amplitude $\sim 0^m.5$, which is also typical an LBV star.

Polcaro et al. [10] used various collections of photographic plates to further extend the historical light curve back to the beginning of the 20th century. The data between 1900 and 1950 suggest that no significant eruption took place during that half century. On the contrary, after 1960, two clear, long-term eruptions are evident (see Figure 2).

New photometric data, collected in Table 3 and shown as magenta dots in Figure 2, confirm the conclusion of Maryeva et al. [22] and Calabresi et al. [29] that the star has reached a long lasting visual minimum phase in 2013, and its brightness has been relatively stable since then.

Table 3. New photometric observations of GR 290 acquired by our group since Polcaro et al. [10].

Date	<i>B</i>		<i>V</i>		<i>R</i>		<i>I</i>		Obs ^a
31 July 2016	18.75	0.03	18.77	0.04	18.59	0.04	18.66	0.05	Loiano
4 August 2016	18.75	0.03	18.77	0.04	18.59	0.04	18.66	0.05	Loiano
29 October 2016			18.60	0.1					ARA
30 October 2016			18.80						Loiano
31 October 2016					18.68	0.15			ARA
28 December 2016			18.78	0.15	18.71	0.15			ARA
16 February 2017	18.70	0.04	18.68	0.04	18.59	0.05	18.73	0.06	Loiano
28 July 2017			18.80	0.04	18.62	0.05			Loiano
30 July 2017			18.87	0.12					ARA
17 December 2017			18.67	0.10					ARA
14 February 2018	18.69	0.05	18.77	0.06	18.64	0.08			RTT-150
19 August 2018			18.81	0.10					ARA
4 September 2018	18.53	0.04	18.67	0.04	18.54	0.04	19.48	0.04	CMO
11 September 2018			18.84	0.04	18.64	0.04			Loiano
13 September 2018	18.65	0.04	18.73	0.04	18.63	0.04	19.51	0.04	CMO
19 September 2018	18.74	0.05	18.83	0.04	18.70	0.04			Loiano
10 January 2019			18.84	0.06	18.74	0.05			Loiano

^a observatories: Loiano: 1.52 m telescope at the Loiano station of the Bologna Astronomical Observatory-INAF. ARA: 37 cm telescope of the Associazione Romana Astrofili at Frasso Sabino (Rieti); RTT-150: 1.5 m Russian–Turkish telescope. CMO: 2.5 m telescope of the Caucasian Mountain Observatory.

It is generally observed that, during the S Dor cycle, the colour of a typical LBV is bluer at the light minimum than close to the light maximum. In contrast, Polcaro et al. [10] demonstrated that $(B - V)$ colour of Romano’s star is constant over time, within the error bars. There is no clear evidence for a variation of $(B - V)$ as a function of the visual magnitude, and our new photometry obtained after 2015 confirms this conclusion (see Figure 3). This is consistent with Romano’s star being hotter (about 30,000 K) than a typical LBV, with the slope of optical spectrum defined by a Raleigh-Jeans power-law tail.

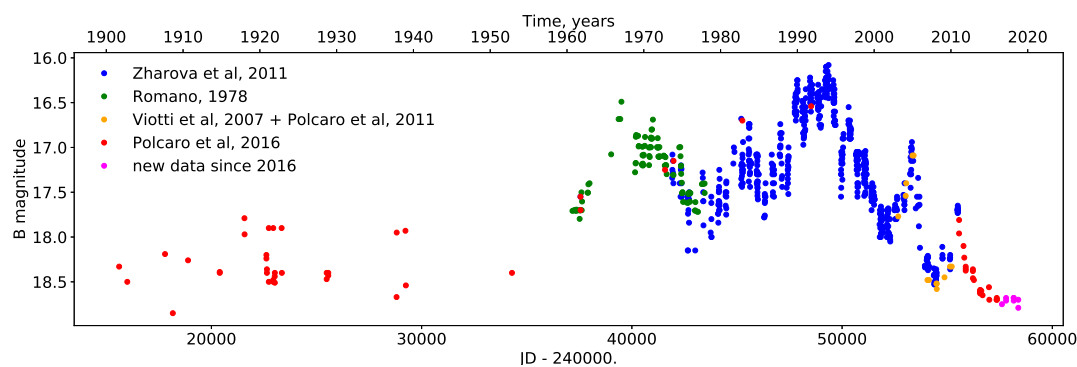


Figure 2. The historical light curve of GR 290 in the B-filter from 1901 to 2019.

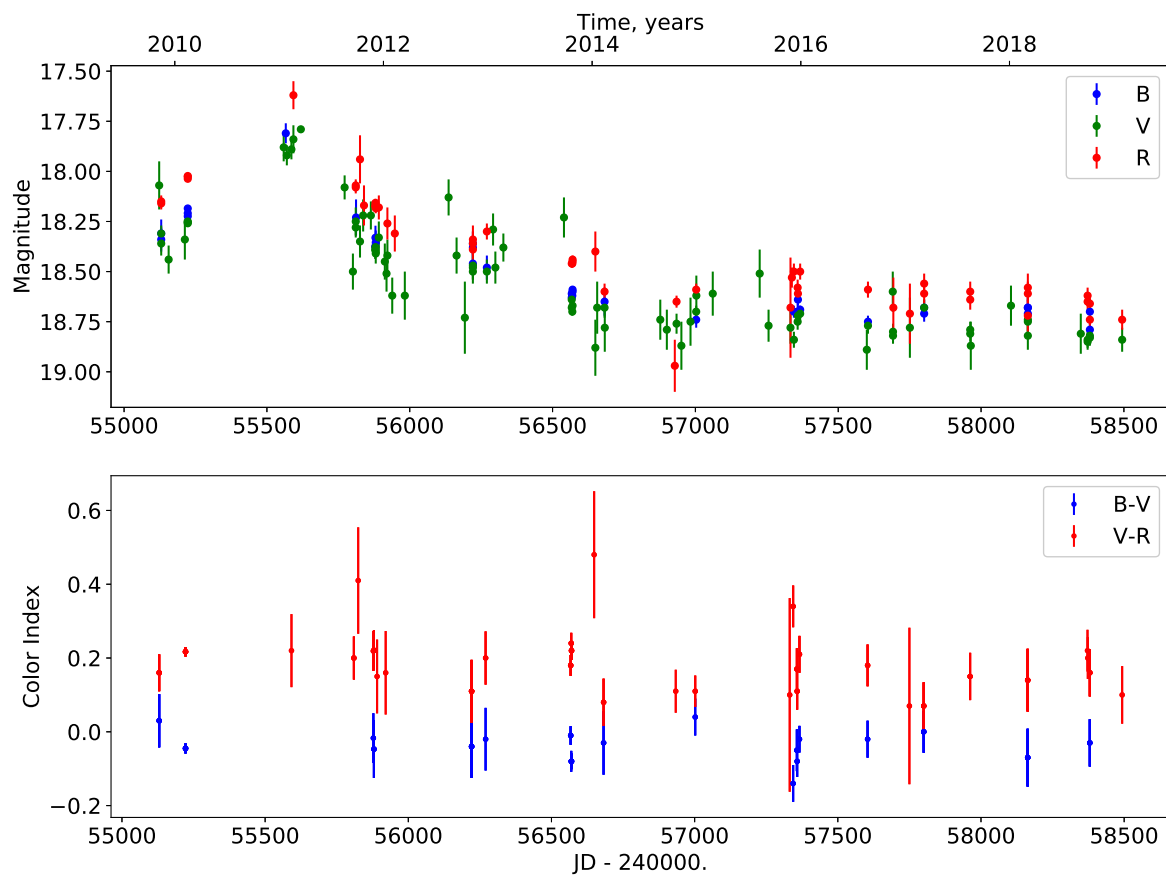


Figure 3. (top) Light curve of GR290 in the B, V and R filters obtained by us between 2010 and 2019 and partially published in Polcaro et al. [10]. (bottom) $(B - V)$ and $(V - R)$ colour indices for the same time interval.

In other spectral ranges, the object is much less studied than in optical range. Only a single measurement of its magnitude is available in ultraviolet and infrared ranges, corresponding to different moments of time defined by a mean epoch of the individual survey (Table 4).

Table 4. Stellar magnitudes of GR290 in ultraviolet and infrared range.

GALEX			2MASS		Spitzer	
Far-UV 1516 Å	Near-UV 2267 Å	J	H	K	3.6 μm	4.5 μm
17.692 ± 0.031	17.438 ± 0.013	16.834 ± 0.128	16.702 ± 0.292	16.657	16.335	15.921
[30]			[31]		[32]	

4. Spectroscopy and Determination of Physical Parameters

The first description of optical spectrum of Romano's star can be found in the article of Humphreys [33]. The spectrum was obtained in August 1978 at Kitt Peak National Observatory, when brightness of the star was $V = 18.00 \pm 0.02$ [33]. Humphreys noted: "Its spectrum shows emission lines of hydrogen and He I. There are no emission lines of Fe II or [Fe II]." and classified the star as a peculiar emission-line object⁶ [33].

⁶ In Humphreys [33], Romano's star is identified as B601.

In 1992, T. Szeifert obtained a spectrum of Romano’s star right before the historical maximum of its brightness. Szeifert [4] described it as “Few metal lines are visible, although a late B spectral type is most likely” (Figure 4). On the other hand, Sholukhova et al. [34] obtained the next spectrum in August 1994 and classified the star as a WN star candidate. Since 1998, regular observations of GR 290 carried out on the Russian 6m [5,35] and spectra published by Sholukhova et al. [35] indicate that the spectrum of GR 290 has not reverted to a B-type spectrum. Thus, Szeifert’s [4] spectrum is unique and corresponds to the coldest and brightest state of the star measured so far.

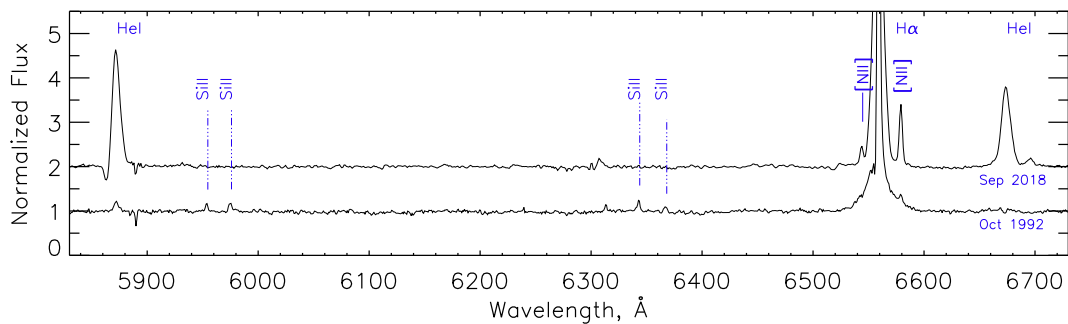


Figure 4. Comparison of normalized optical spectra of GR 290 obtained with Calar Alto/TWIN in October 1992 by Szeifert [4] and with GTC/OSIRIS in September 2018. Spectra are displaced vertically for illustrative purposes.

Studies of GR 290 devoted to its spectral variability show that its spectral type changes between WN11 and WN8 [8,35,36]. Since the beginning of the 2000s, it has made this transition twice [10]. Viotti et al. [37,38] first described an anticorrelation between equivalent width of 4600–4700 Å blend and the brightness. Later, Maryeva and Abolmasov [36] found a correlation of spectral changes and the visual brightness typical for LBVs: the brighter it is, the cooler the spectral type. However, as noted by Humphreys et al. [9], GR 290 does not exhibit S Dor like transitions to the cool state with an optically thick wind, but instead varies between two hot states characterised by WN spectroscopic features. Among all known LBVs, only HD 5980 [39] convincingly shows a hotter spectrum in the minimum of brightness. Other LBV stars showing WN-like spectrum in quiescent “hot” phase usually stop at colder spectral types such as WN11 (for example AG Car [40] and WS 1 [41,42]) or Ofpe/WN9 (for example R 127 [43] and HD 269582 [44]).

As already mentioned, since the autumn of 2013, GR 290 is in a minimum brightness state with $V = 18.7\text{--}18.8$ mag. Due to this, it has been challenging to obtain its spectra with good enough quality for wind speeds to be adequately estimated. In summer of 2016, GR 290 was observed with the Optical System for Imaging and low-Intermediate-Resolution Integrated Spectroscopy (OSIRIS) on the *Gran Telescopio Canarias* (GTC) [22]. These observations gave the best spectral resolutions and signal-to-noise ratios ever obtained for this object, and allowed to estimate an average radial velocity (RV) of the object, $RV(\text{GR 290}) = -163 \pm 32 \text{ km s}^{-1}$, which is consistent, within the uncertainties, with the heliocentric velocity $-179 \pm 3 \text{ km s}^{-1}$ of M33 galaxy.

New spectra of GR 290 were obtained with the OSIRIS spectrograph in September 2018 [23]. Detailed analysis of the spectra obtained in 2016 and 2018 did not reveal any changes (Figure 5). As before, the star displays a WN8h spectrum with forbidden nebular lines.

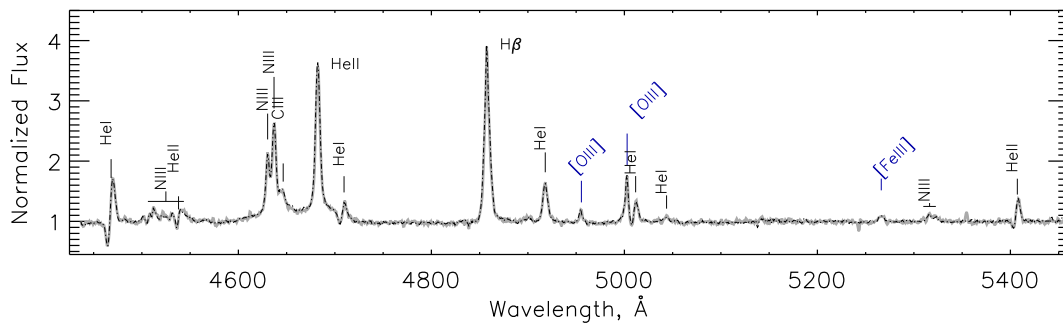


Figure 5. Comparison of normalised optical spectra of GR 290 obtained with GTC/OSIRIS in July 2016 (grey thick line) and September 2018 (black dash-dotted line). Spectra are nearly identical.

The large number of acquired spectra allows tracking the quantitative changes of physical parameters of the star over time. To do it, a numerical modeling of GR 290's atmosphere using CMFGEN code [45] was started by Maryeva and Abolmasov [46], who constructed models for two states—the luminosity maximum of 2005 and the minimum of brightness in 2008. Then, Clark et al. [47] estimated the parameters of GR 290 during the moderate luminosity maximum of 2010. Polcaro et al. [10] built nine models for the most representative spectra acquired between 2002 and 2014. The results of calculations from Polcaro et al. [10], Clark et al. [47] and Maryeva et al. [22] are summarised in Table 5, along with the parameters estimated using the spectrum of September 2018. Comparisons of observed spectra with corresponding models are shown in Figure 6.

Table 5. Derived properties of Romano's star at the moments corresponding to different acquired spectra. H/He indicates the hydrogen number fraction relative to helium, f is the filling factor of the stellar wind. Details of modeling may be found in [10,22,47].

Date	V [mag]	Sp. type	T_{eff} [kK]	$\log T_{\text{eff}}$	$R_{2/3}$ [R_{\odot}]	$L_{*}10^5$ [L_{\odot}]	$\log L_{*}$ [L_{\odot}]	$\dot{M}_{cl}10^{-5}$ [M_{\odot}/yr]	f	v_{∞} [km/s]	H/He	Ref.
Oct. 2002	17.98	WN10h	28.1	4.45	31.6	5.6	5.75	1.9	0.15	250 ± 100	1.7	[10]
Feb. 2003	17.70	WN10.5h	28.0	4.45	37	7.5	5.875	2.2	0.15	250 ± 50	1.7	[10]
Jan. 2005	17.24	WN11h	23.6	4.37	54	8.2	5.91	3.5	0.15	250 ± 50	1.7	[10]
Sep. 2006	18.4	WN8h	30.7	4.49	24	4.6	5.66	1.3	0.15	250 ± 100	1.7	[10]
Oct. 2007	18.6	WN8h	33.5	4.53	20	4.5	5.65	1.55	0.15	370 ± 50	1.7	[10]
Dec. 2008	18.31	WN8h	31.6	4.50	23.5	5.0	5.7	1.9	0.15	370 ± 50	1.7	[10]
Oct. 2009	18.36	WN9h	31.6	4.50	23.8	5.1	5.7	1.7	0.15	300 ± 100	1.7	[10]
Sep. 2010 ^a	17.8	WN10h	26	4.41	41.5		5.85	2.18	0.25	265	1.5	[47]
Dec. 2010	17.95	WN10h	26.9	4.43	33	5.3	5.72	2.05	0.15	250 ± 100	1.7	[10]
Aug. 2014	18.74	WN8h	32.8	4.52	19	3.7	5.57	1.4	0.15	400 ± 100	1.7	[10]
Jul. 2016	18.77	WN8h	30.0	4.48	21	3.7	5.57	1.5	0.15	620 ± 50	2.2	[22]
Sep. 2018	18.77	WN8h	30.0	4.48	21	3.7	5.57	1.5	0.15	620 ± 50	2.2	

^a Clark et al. [47] assumed a distance to M 33 of 964 kpc.

Numerical calculations show that the bolometric luminosity of GR 290 is variable, being higher during the phases of greater optical brightness [10,46]. At the same time, the wind structure of GR 290 also varies in correlation with brightness changes—the slow and dense wind at brightness maxima becomes faster and thinner at minima (Figure 7), and the effective temperature⁷ of the star increases from 25 kK (with WN11h spectral type) during the maximum of 2005 year to 31–33 kK (WN8h) during the minima.

⁷ Effective temperature is defined as a temperature at radius $R_{2/3}$, where the Rosseland optical depth is equal to 2/3.

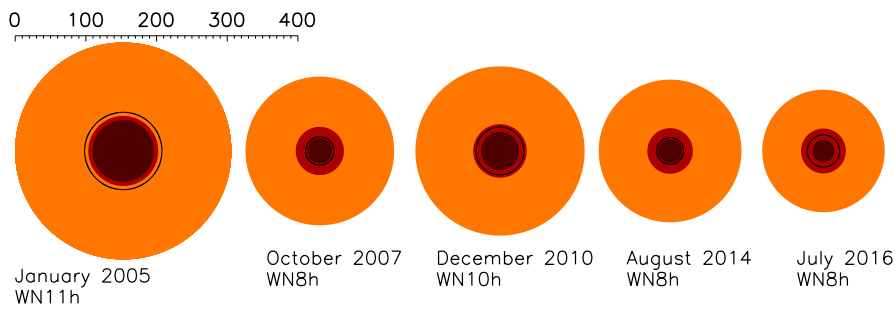


Figure 7. Change of the wind structure and extent over time. The region where $n_e \geq 10^{12} \text{ cm}^{-3}$ is shown in dark red, $10^{12} \geq n_e \geq 10^{11} \text{ cm}^{-3}$ in red, and $10^{11} \geq n_e \geq 10^{10} \text{ cm}^{-3}$ in orange. Solid black line shows the radius where Rosseland optical depth (τ) is $2/3$. Scale in units R_\odot is shown at the top.

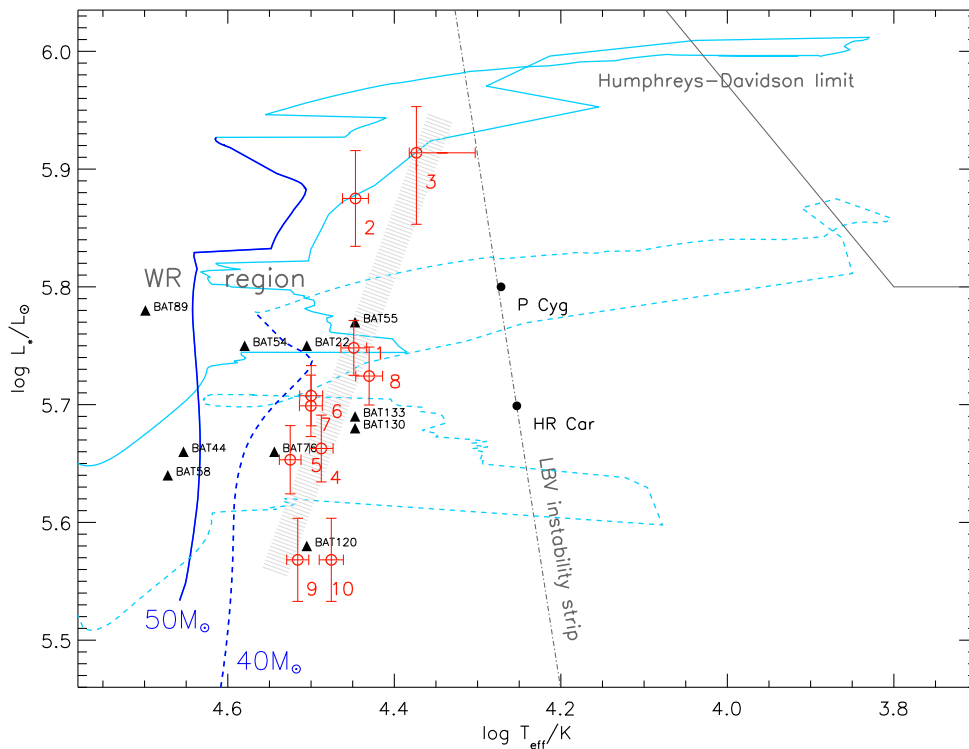


Figure 8. Position of GR290 in the Hertzsprung-Russell diagram at different times. Numbers correspond to: (1) October 2002; (2) February 2003; (3) January 2005; (4) September 2006; (5) October 2007; (6) December 2008; (7) October 2009; (8) December 2010; (9) August 2014; and (10) July 2016 and September 2018. The hatched strip shows an average line along which GR 290 moved during its recent luminosity cycles. The Geneva tracks [51] for $40 M_\odot$ (dashed line) and $50 M_\odot$ (solid line) with rotation are shown by blue lines, with dark blue part corresponding to the hydrogen burning in stellar core. Triangles mark the positions of late-WN stars from Large Magellanic Cloud (LMC), whose data were taken from Hainich et al. [52]. In addition, the positions of LBV stars P Cygni and HR Car are shown with circles. Data for these objects were taken from the works of Najarro [53] and Groh et al. [54]. Grey solid line is Humphreys-Davidson limit [3], grey dash-dotted line is LBV minimum instability strip as defined in [54].

5. Nebula

The presence of forbidden lines [N II] 6548, 6584; [O III] 4959, 5007; [Fe III] 4658, 4701, 5270 and [Ar III] 7136 in the spectrum of GR 290 indicates that it has a nebula, but it is not resolved in direct

imaging because of the large distance to M33. In 2005, Fabrika et al. [5] first attempted to detect the nebula and study its spatial structure using the panoramic (3D) spectroscopic data acquired on Russian 6-m telescope, and reported the discovery of an extended structure in the velocity field of H β line, with an angular extent of $\sim 9''$ (~ 30 pc) in the NE-SW direction. An excess corresponding to the dust circumstellar envelope around the object has not been detected in the infrared (IR) emission [9].

Maryeva et al. [22] performed a modeling of circumstellar nebula using CLOUDY photoionisation code [55,56] and the spectrum acquired on GTC/OSIRIS in order to reproduce the observed nebular emission lines that are clearly seen in the spectrum. GR 290 was found to be surrounded by an unresolved compact H II region with a most probable outer radius $R = 0.8$ pc and a hydrogen density $n_H = 160 \text{ cm}^{-3}$, and having chemical abundances that are consistent with those derived from the stellar wind lines. Hence, this compact H II region appears to be largely composed of material ejected from the star.

In addition, the recent analysis of the 2D spectra obtained with GTC/OSIRIS in September 2018 perpendicular to the dispersion at H α line indicates that the nebula has extended and asymmetric structure [23]. Its size is about 25–30 pc, similar to typical H II regions around O-stars. Based on the similarity of sizes and evolutionary status of GR 290, we speculate that this extended nebula consists of material ejected during O-supergiant phase.

6. Conclusions

GR 290 is located in the outer spiral arm of the M33 galaxy at a projected distance of about 4 kpc from the centre. Its spatial location, the proximity to the OB 88 and OB 89 associations, and the similarity of their ages (about 4–5 Myr) as well as a basic concept that a large fraction of all stars, including massive stars, forms in clusters suggest the common origin of GR 290 and OB 89. It is tempting to suggest that GR 290 may have escaped from the association.

The evolution of LBVs during the S Dor cycles seems to occur in most cases roughly at constant bolometric luminosity (see, e.g., [3,57]). However, a decrease of bolometric luminosity from minimum towards the light maximum of the S Dor cycle were observed for several LBVs (e.g., S Dor [58] and AG Car [40]). Lamers [58] interpreted it in terms of the radiative power being partially transformed into mechanical power in order to expand the outer layers of the star from minimum to maximum. In contrast, spectral monitoring of Romano's star during its recent peaks of activity, and the numerical simulation of its stellar atmosphere based on acquired spectra, demonstrated that its bolometric luminosity varies in correlation with its visual brightness, i.e., L_{bol} increases during its visual luminosity maxima [10]. Guzik and Lovekin [59] discussed several mechanisms that could trigger the large outburst activity and variations in bolometric magnitude as observed in GR 290. An interesting possibility is that the interplay between pulsations and rotational mixing lead to an unstable transport of H-rich material to the nuclear burning core. In this context, GR 290 may be the ideal object for testing such theories.

The star is hotter than most other LBVs (Table 6), and lays outside of the LBV instability strip in the H-R diagram. On the other hand, the hydrogen abundance of the envelope appears higher than in late type WN stars, and therefore, from the evolutionary and structural point of view, GR 290 is less evolved than WN8h stars [10]. This suggests that Romano's star may be a post-LBV object, the transition phase between LBVs and Wolf-Rayet stars.

The century long light curve of Romano's star shows that until the 1960s the object was in a long lasting quasi-stationary state, a state to which it has returned in 2013, and since then displaying a WN8h spectrum. While the spectral type during the early "low" state (pre-1960) is unknown, from the observed correlation between the visual magnitude and spectral type, we may suggest that it also was WN8h. The Galactic WN8 stars are known to be significantly more variable than the WRs with hotter spectral types [60]. Thus, it is tempting to speculate on the possibility that, in analogy with GR 290, other WN8s may have just recently passed through the LBV phase. Hence, a systematic

investigation of archival data and constructing century long light curves for WN8-WN9 stars using archival photographic plates will probably be able to uncover more objects similar to Romano's star.

Table 6. Comparison of Romano's star with other LBVs and LBV candidates which show WR like spectra.

Star	Sp.type	Ref.	Comments
Wray 15-751	O9.5 I	[61]	LBVc, Milky Way
Sk-69° 279	O9.2 Iaf	[62]	ex-/dormant LBV [63], BSG evolved off the Main Sequence [62]
Hen 3-519	WN11	[64]	ex-/dormant LBV [63], there are no significant changes of brightness [65]
AG Car	WN11	[40]	LBV, Milky Way
WS 1	WN11	[41,42]	LBV, Milky Way
R 127	Ofpe/WN9	[43]	LBV, Large Magellanic Cloud
HD 269582	Ofpe/WN9	[44]	LBV, Large Magellanic Cloud
GR 290	WN8	[10,22]	post-LBV, M33
HD 5980	LBV+WN4+OI	[66,67]	LBV, Small Magellanic Cloud

Author Contributions: R.F.V., spectral analysis; M.C., C.R. and R.G., photometric monitoring and reduction of photometry data; and O.M., numerical modeling of stellar atmosphere and reduced the spectroscopic material and manuscript preparation. G.K. was PI of the 2016 and 2018 GranTeCan observations and performed spectral analysis. All authors discussed the results and commented on the manuscript.

Funding: This research was funded by CONACYT grant 252499, UNAM/PAPIIT grant IN103619, Russian Foundation for Basic Research grant 19-02-00779 and Czech Science Foundation grant GA18-05665S. This project received funding from the European Union's Framework Programme for Research and Innovation Horizon 2020 (2014-2020) under the Marie Skłodowska-Curie Grant Agreement No. 823734.

Acknowledgments: We express our enormous gratitude to V.F. Polcaro, who recently passed away, for having stimulated our interest and studies of this unique object. We thank Roman Zhuchkov, Oleg Egorov and Olga Vozyakova for obtaining the photometric observations on 1.5 m Russian–Turkish telescope and 2.5 m telescope of the Caucasian Mountain Observatory. We thank Thomas Szeifert and Philip Massey for the spectra obtained with Calar Alto/TWIN spectrograph in 1992 and with WIYN 3.5 m telescope in September 2006. We thank the GTC observatory staff for obtaining the spectra and Antonio Cabrera-Lavers for guidance in processing the observations. We thank Guest Editor Prof. Roberta M. Humphreys and our anonymous referees for providing helpful comments and suggestions. In this paper, we use data taken from the public archive of the SAO RAS. The work is partially based on the observation at 2.5-m CMO telescope that is supported by M.V. Lomonosov Moscow State University Program of Development.

Conflicts of Interest: The authors declare no conflict of interest.

Abbreviations

The following abbreviations are used in this manuscript:

CMO	2.5 m telescope of the Caucasian Mountain Observatory of the Sternberg Astronomical Institute of Moscow State University
GTC	Gran Telescopio Canarias
LBV	Luminous blue variable
BSG	Blue supergiant
RSG	Red supergiant
SAO RAS	Special Astrophysical observatory of Russian Academy of Sciences
WR	Wolf-Rayet
WN	Nitrogen-rich Wolf-Rayet stars
WC	Carbon-rich Wolf-Rayet stars
YHG	Yellow hypergiant

Appendix A. Spectra of Stars in Vicinity of GR 290

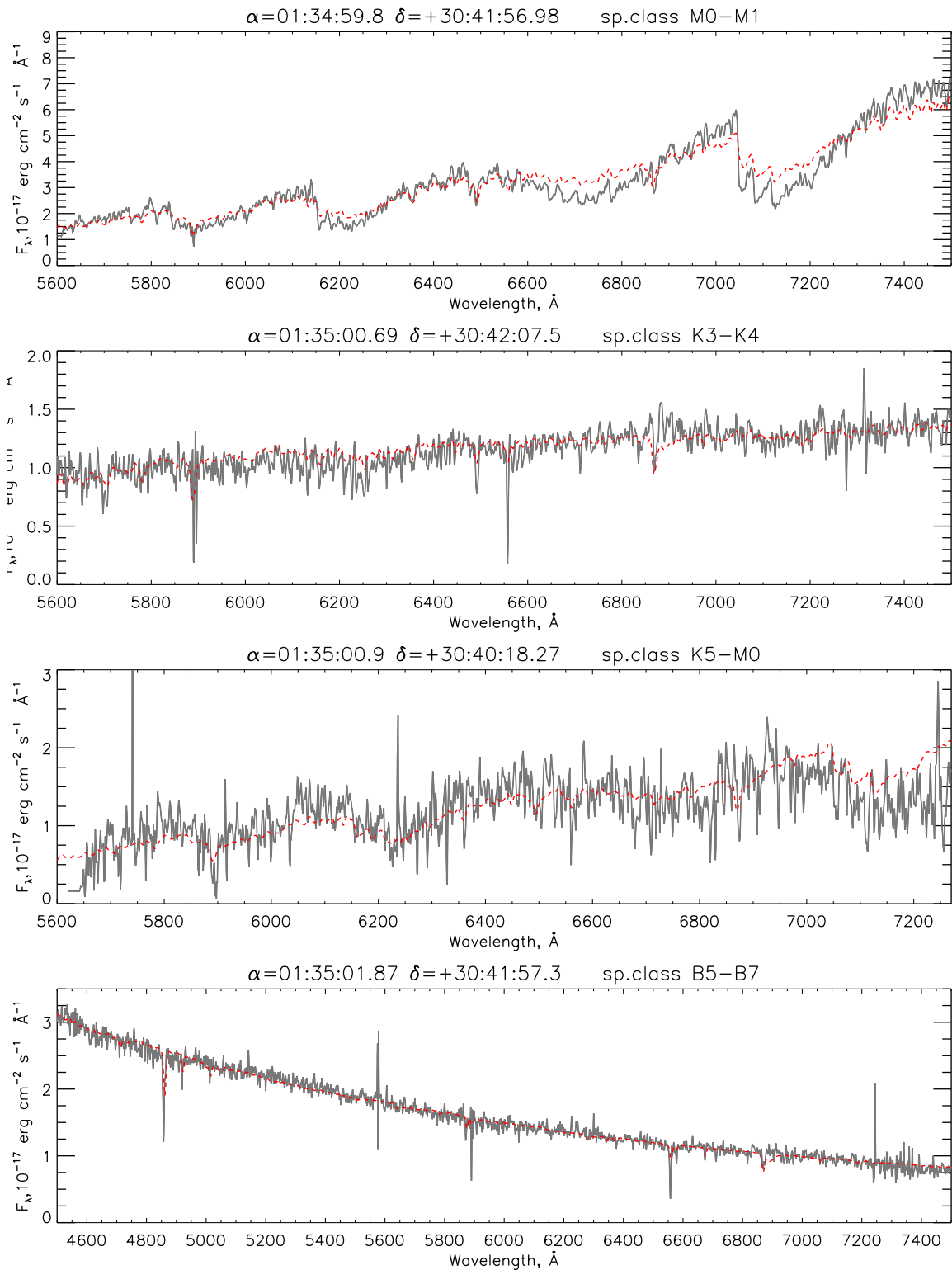


Figure A1. From the top panel downwards, spectra of the stars: J013459.8+304156.98, J013500.69+304207.5, J013500.9+304018.27 and J013501.87+304157.3. For comparison, the reddened spectra of HD 42543 (M1 Ia-ab), HD 154733 (K3 III), HD 146051 (M0.5 III) and HD 164353 (B5 Ib) are shown by red dashed lines.

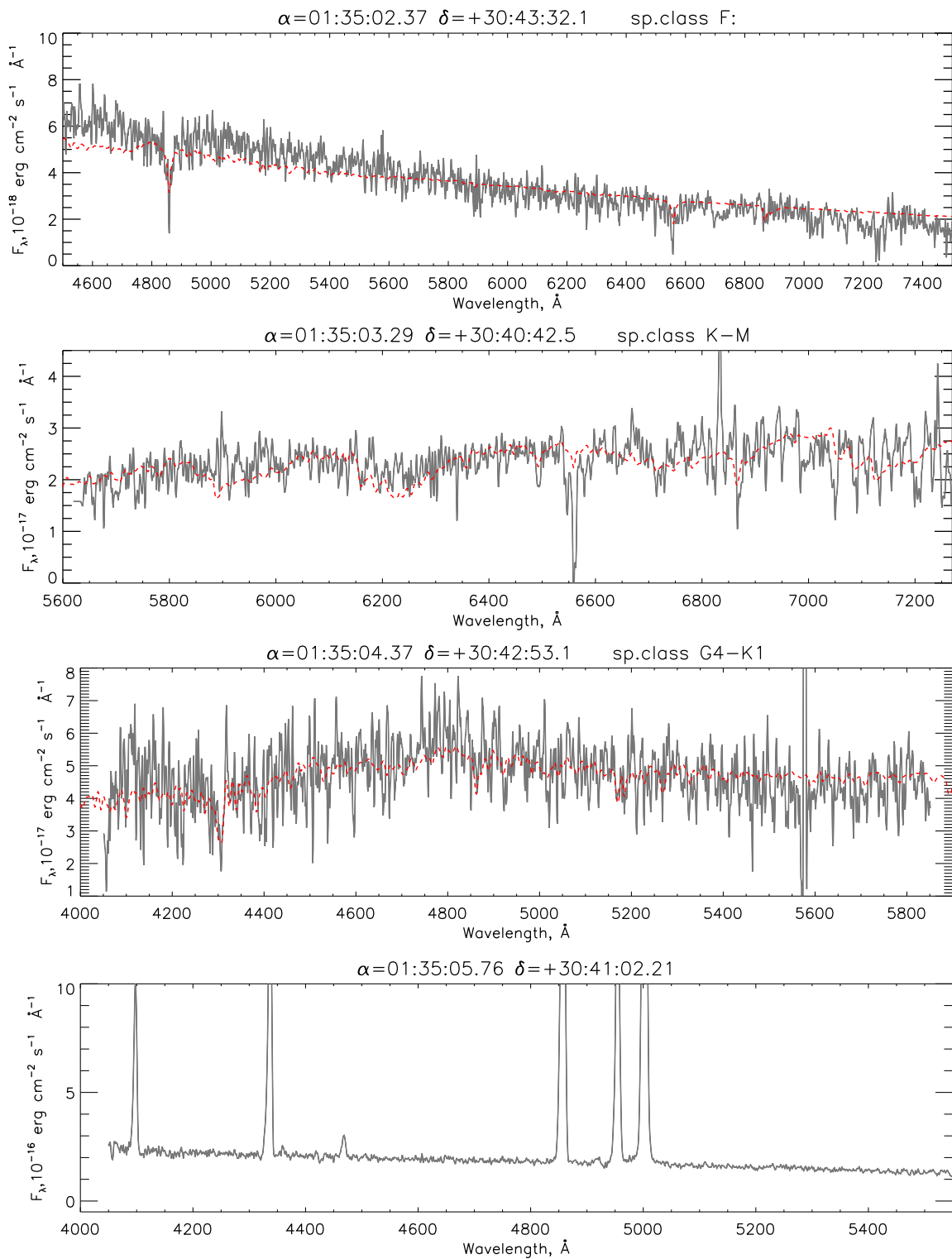


Figure A2. From the top panel downwards, spectra of the stars: J013502.37+304332.1, J013503.29+304042.5, J013504.37+304253.1 and J013505.76+304102.21. For comparison, the reddened spectra of HD 128167 (F2 V), HD 102212 (M1 III) and HD 135722 (G8 III) are shown by red dashed lines.

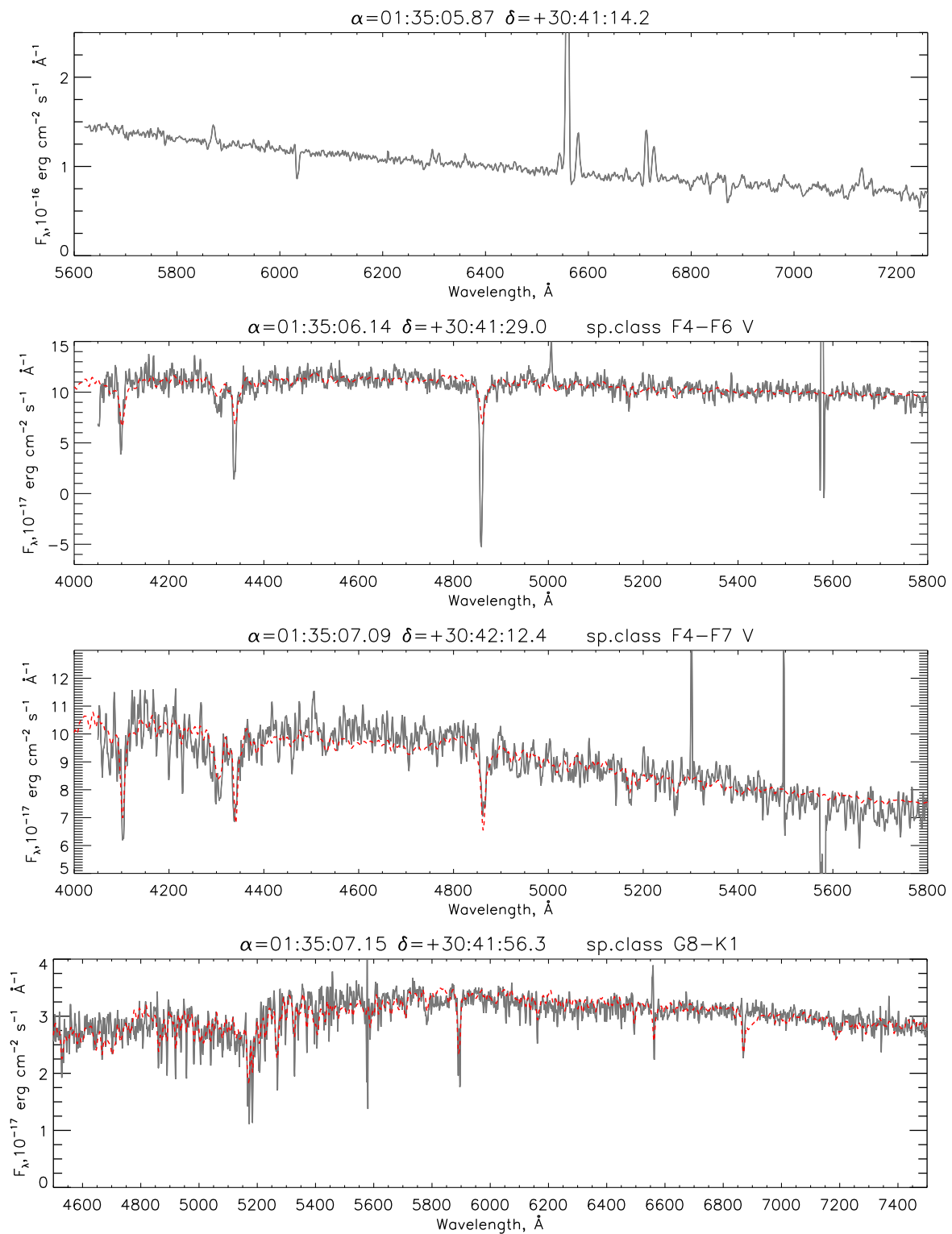


Figure A3. From the top panel downwards, spectra of the stars: J013505.87+304114.2, J013506.14+304129.0, J013507.09+304212.4 and J013507.15+304156.3. For comparison, the reddened spectra of HD 126141 (F5 V), HD 101606 (F4 V) and HD 75532 (G8 V) are shown by red dashed lines.

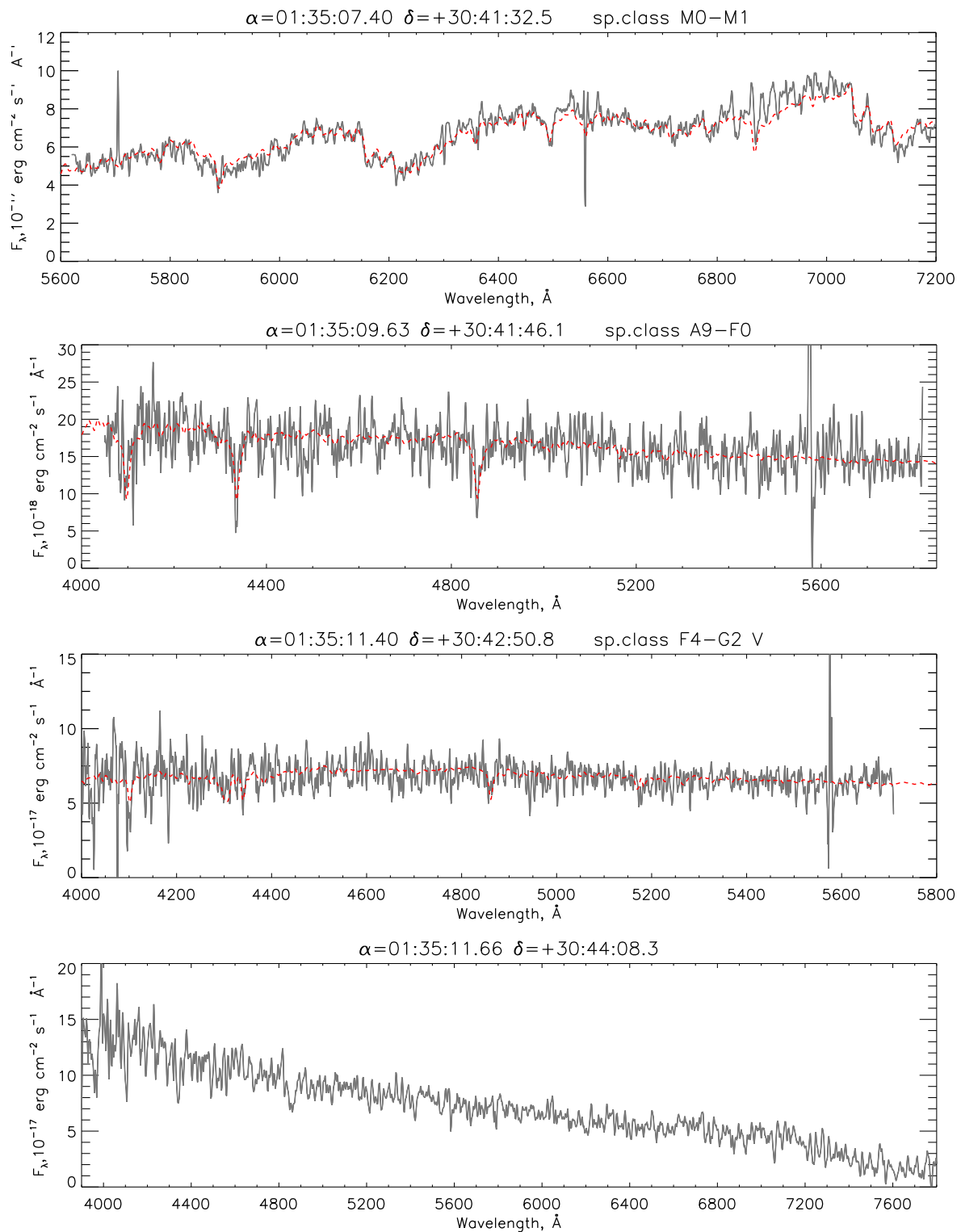


Figure A4. From the top panel downwards, spectra of the stars: J013507.40+304132.5, J013509.63+304146.1, J013511.40+304250.8 and J013511.66+304408.3. For comparison, the reddened spectra of HD 146051 (M0.5 III), HD 50420 (A9 III) and HD 134169 (G1 V) are shown by red dashed lines.

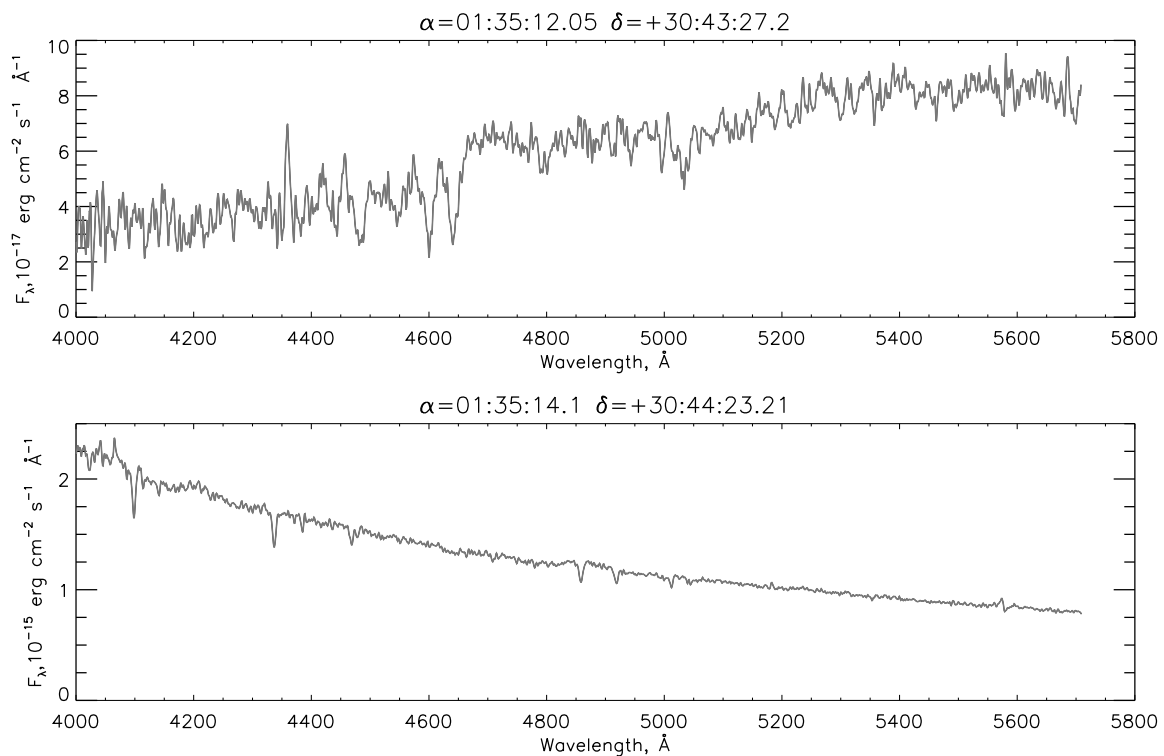


Figure A5. From the top panel downwards, spectra of the stars: J013512.05+304327.2 and J013514.1+304423.21.

References

1. Romano, G. A new variable star in M33. *Astron. Astrophys.* **1978**, *67*, 291–292.
2. Conti, P.S. Basic Observational Constraints on the Evolution of Massive Stars. In *Symposium-International Astronomical Union; Observational Tests of the Stellar Evolution Theory*; Maeder, A., Renzini, A., Eds.; Cambridge University Press: Cambridge, UK, 1984; Volume 105, p. 233.
3. Humphreys, R.M.; Davidson, K. The luminous blue variables: Astrophysical geysers. *Publ. ASP* **1994**, *106*, 1025–1051. [[CrossRef](#)]
4. Szeifert, T. LBVs and a late WN-star in M 31 and M 33. In *Liège International Astrophysical Colloquia*; Vreux, J.M., Detal, A., Fraipont-Caro, D., Gosset, E., Rauw, G., Eds.; Université de Liège. Institut d’astrophysique: Liège, Belgium, 1996; Volume 33, p. 459.
5. Fabrika, S.; Sholukhova, O.; Becker, T.; Afanasiev, V.; Roth, M.; Sanchez, S.F. Crowded field 3D spectroscopy of LBV candidates in M 33. *Astron. Astrophys.* **2005**, *437*, 217–226. [[CrossRef](#)]
6. Kurtev, R.; Sholukhova, O.; Borissova, J.; Georgiev, L. Romano’s Star in M33: LBV Candidate or LBV? *Rev. Mex.* **2001**, *37*, 57–61.
7. Polcaro, V.F.; Gualandi, R.; Norci, L.; Rossi, C.; Viotti, R.F. The LBV nature of Romano’s star (GR 290) in M 33. *Astron. Astrophys.* **2003**, *411*, 193–196. [[CrossRef](#)]
8. Polcaro, V.F.; Rossi, C.; Viotti, R.F.; Galleti, S.; Gualandi, R.; Norci, L. Optical Spectrophotometric Monitoring of the Extreme Luminous Blue Variable Star GR 290 (Romano’s Star) in M 33. *Astron. J.* **2011**, *141*, 18. [[CrossRef](#)]
9. Humphreys, R.M.; Weis, K.; Davidson, K.; Bomans, D.J.; Burggraf, B. Luminous and Variable Stars in M31 and M33. II. Luminous Blue Variables, Candidate LBVs, Fe II Emission Line Stars, and Other Supergiants. *Astrophys. J.* **2014**, *790*, 48. [[CrossRef](#)]
10. Polcaro, V.F.; Maryeva, O.; Nesci, R.; Calabresi, M.; Chieffi, A.; Galleti, S.; Gualandi, R.; Haver, R.; Mills, O.F.; Osborn, W.H.; Pasquali, A.; Rossi, C.; Vasilyeva, T.; Viotti, R.F. GR 290 (Romano’s Star). II. Light History and Evolutionary State. *Astron. J.* **2016**, *151*, 149. [[CrossRef](#)]

11. Humphreys, R.M.; Sandage, A. On the stellar content and structure of the spiral Galaxy M33. *Astrophys. J. Suppl. Ser.* **1980**, *44*, 319–381. [[CrossRef](#)]
12. Ivanov, G.R.; Freedman, W.L.; Madore, B.F. A catalog of blue and red supergiants in M33. *Astrophys. J. Suppl. Ser.* **1993**, *89*, 85–122. [[CrossRef](#)]
13. Massey, P.; Armandroff, T.E.; Pyke, R.; Patel, K.; Wilson, C.D. Hot, Luminous Stars in Selected Regions of NGC 6822, M31, and M33. *Astron. J.* **1995**, *110*, 2715. [[CrossRef](#)]
14. Galleti, S.; Bellazzini, M.; Ferraro, F.R. The distance of M 33 and the stellar population in its outskirts. *Astron. Astrophys.* **2004**, *423*, 925–934. [[CrossRef](#)]
15. Massey, P.; Neugent, K.F.; Smart, B.M. A Spectroscopic Survey of Massive Stars in M31 and M33. *Astron. J.* **2016**, *152*, 62. [[CrossRef](#)]
16. Massey, P.; Olsen, K.A.G.; Hodge, P.W.; Strong, S.B.; Jacoby, G.H.; Schlingman, W.; Smith, R.C. A Survey of Local Group Galaxies Currently Forming Stars. I. UBVRI Photometry of Stars in M31 and M33. *Astron. J.* **2006**, *131*, 2478–2496. [[CrossRef](#)]
17. Massey, P.; Johnson, O. Evolved Massive Stars in the Local Group. II. A New Survey for Wolf-Rayet Stars in M33 and Its Implications for Massive Star Evolution: Evidence of the “Conti Scenario” in Action. *Astrophys. J.* **1998**, *505*, 793–827. [[CrossRef](#)]
18. Massey, P.; McNeill, R.T.; Olsen, K.A.G.; Hodge, P.W.; Blaha, C.; Jacoby, G.H.; Smith, R.C.; Strong, S.B. A Survey of Local Group Galaxies Currently Forming Stars. III. A Search for Luminous Blue Variables and Other H α Emission-Line Stars. *Astron. J.* **2007**, *134*, 2474–2503. [[CrossRef](#)]
19. Perets, H.B.; Šubr, L. The Properties of Dynamically Ejected Runaway and Hyper-runaway Stars. *Astrophys. J.* **2012**, *751*, 133. [[CrossRef](#)]
20. Humphreys, R.M.; Gordon, M.S.; Martin, J.C.; Weis, K.; Hahn, D. Luminous and Variable Stars in M31 and M33. IV. Luminous Blue Variables, Candidate LBVs, B[e] Supergiants, and the Warm Hypergiants: How to Tell Them Apart. *Astrophys. J.* **2017**, *836*, 64. [[CrossRef](#)]
21. Afanasiev, V.L.; Moiseev, A.V. The SCORPIO Universal Focal Reducer of the 6-m Telescope. *Astron. Lett.* **2005**, *31*, 194–204. [[CrossRef](#)]
22. Maryeva, O.; Koenigsberger, G.; Egorov, O.; Rossi, C.; Polcaro, V.F.; Calabresi, M.; Viotti, R.F. Wind and nebula of the M 33 variable GR 290 (WR/LBV). *Astron. Astrophys.* **2018**, *617*, A51. [[CrossRef](#)]
23. Maryeva, O.; Koenigsberger, G.; Karpov, S.; Lozinskaya, T.; Egorov, O.; Rossi, C.; Calabresi, M.; Viotti, R.F. Asymmetrical nebulae of the M33 variable GR 290 (WR/LBV). 2019, in preparation.
24. Le Borgne, J.F.; Bruzual, G.; Pelló, R.; Lançon, A.; Rocca-Volmerange, B.; Sanahuja, B.; Schaerer, D.; Soubiran, C.; Vílchez-Gómez, R. STELIB: A library of stellar spectra at R~2000. *Astron. Astrophys.* **2003**, *402*, 433–442. [[CrossRef](#)]
25. Maryeva, O.V.; Chentsov, E.L.; Goranskij, V.P.; Dyachenko, V.V.; Karpov, S.V.; Malogolovets, E.V.; Rastegaev, D.A. On the nature of high reddening of Cygnus OB2 #12 hypergiant. *Mon. Not. R. Astron. Soc.* **2016**, *458*, 491–507. [[CrossRef](#)]
26. Schlegel, D.J.; Finkbeiner, D.P.; Davis, M. Maps of Dust Infrared Emission for Use in Estimation of Reddening and Cosmic Microwave Background Radiation Foregrounds. *Astrophys. J.* **1998**, *500*, 525–553. [[CrossRef](#)]
27. Zharova, A.; Goranskij, V.; Sholukhova, O.N.; Fabrika, S.N. V532 in M33. *Peremennye Zvezdy Prilozhenie* **2011**, *11*, 11.
28. Abolmasov, P. Stochastic variability of luminous blue variables. *New Astron.* **2011**, *16*, 421–429. [[CrossRef](#)]
29. Calabresi, M.; Rossi, C.; Gualandi, R.; Galleti, S.; Polcaro, V.F.; Viotti, R.; Albanesi, R.; Anzellini, F.; Haver, R.; Caponetto, P.; Gorelli, R. New deep minimum of Romano’s Star in M33. *Astron. Teleg.* **2014**, *5846*, 1.
30. Mudd, D.; Stanek, K.Z. GALEX catalogue of UV point sources in M33. *Mon. Not. R. Astron. Soc.* **2015**, *450*, 3811–3821. [[CrossRef](#)]
31. Skrutskie, M.F.; Cutri, R.M.; Stiening, R.; Weinberg, M.D.; Schneider, S.; Carpenter, J.M.; Beichman, C.; Capps, R.; Chester, T.; Elias, J.; et al. The Two Micron All Sky Survey (2MASS). *Astron. J.* **2006**, *131*, 1163–1183. [[CrossRef](#)]
32. McQuinn, K.B.W.; Woodward, C.E.; Willner, S.P.; Polomski, E.F.; Gehrz, R.D.; Humphreys, R.M.; van Loon, J.T.; Ashby, M.L.N.; Eicher, K.; Fazio, G.G. The M33 Variable Star Population Revealed by Spitzer. *Astrophys. J.* **2007**, *664*, 850–861. [[CrossRef](#)]
33. Humphreys, R.M. Studies of luminous stars in nearby galaxies. VI. The brightest supergiants and the distance to M 33. *Astrophys. J.* **1980**, *241*, 587–597. [[CrossRef](#)]

34. Sholukhova, O.N.; Fabrika, S.N.; Vlasjuk, V.V.; Burenkov, A.N. Spectroscopy of H α -emission blue stars in M33. *Astron. Lett.* **1997**, *23*, 458–464. [[CrossRef](#)]
35. Sholukhova, O.N.; Fabrika, S.N.; Zharova, A.V.; Valeev, A.F.; Goranskij, V.P. Spectral variability of LBV star V 532 (Romano’s star). *Astrophys. Bull.* **2011**, *66*, 123–143. [[CrossRef](#)]
36. Maryeva, O.; Abolmasov, P. Spectral Variability of Romano’s Star. *Rev. Mex.* **2010**, *46*, 279–290.
37. Viotti, R.F.; Rossi, C.; Polcaro, V.F.; Montagni, F.; Gualandi, R.; Norci, L. The present status of four luminous variables in M 33. *Astron. Astrophys.* **2006**, *458*, 225–234. [[CrossRef](#)]
38. Viotti, R.F.; Galleti, S.; Gualandi, R.; Montagni, F.; Polcaro, V.F.; Rossi, C.; Norci, L. The 2006 hot phase of Romano’s star (GR 290) in M 33. *Astron. Astrophys.* **2007**, *464*, L53–L55. [[CrossRef](#)]
39. Georgiev, L.; Koenigsberger, G.; Hillier, D.J.; Morrell, N.; Barbá, R.; Gamen, R. Wind Structure and Luminosity Variations in the Wolf-Rayet/Luminous Blue Variable HD 5980. *Astron. J.* **2011**, *142*, 191. [[CrossRef](#)]
40. Groh, J.H.; Hillier, D.J.; Daminieli, A.; Whitelock, P.A.; Marang, F.; Rossi, C. On the Nature of the Prototype Luminous Blue Variable Ag Carinae. I. Fundamental Parameters During Visual Minimum Phases and Changes in the Bolometric Luminosity During the S-Dor Cycle. *Astrophys. J.* **2009**, *698*, 1698–1720. [[CrossRef](#)]
41. Kniazev, A.Y.; Gvaramadze, V.V.; Berdnikov, L.N. WS1: one more new Galactic bona fide luminous blue variable. *Mon. Not. R. Astron. Soc.* **2015**, *449*, L60–L64. [[CrossRef](#)]
42. Gvaramadze, V.V.; Kniazev, A.Y.; Miroshnichenko, A.S.; Berdnikov, L.N.; Langer, N.; Stringfellow, G.S.; Todt, H.; Hamann, W.R.; Grebel, E.K.; Buckley, D.; et al. Discovery of two new Galactic candidate luminous blue variables with Wide-field Infrared Survey Explorer. *Mon. Not. R. Astron. Soc.* **2012**, *421*, 3325–3337. [[CrossRef](#)]
43. Walborn, N.R.; Stahl, O.; Gamen, R.C.; Szeifert, T.; Morrell, N.I.; Smith, N.; Howarth, I.D.; Humphreys, R.M.; Bond, H.E.; Lennon, D.J. A Three-Decade Outburst of the LMC Luminous Blue Variable R127 Draws to a Close. *Astrophys. J. Lett.* **2008**, *683*, L33. [[CrossRef](#)]
44. Walborn, N.R.; Gamen, R.C.; Morrell, N.I.; Barbá, R.H.; Fernández Lajús, E.; Angeloni, R. Active Luminous Blue Variables in the Large Magellanic Cloud. *Astron. J.* **2017**, *154*, 15. [[CrossRef](#)]
45. Hillier, D.J.; Miller, D.L. The Treatment of Non-LTE Line Blanketing in Spherically Expanding Outflows. *Astrophys. J.* **1998**, *496*, 407–427. [[CrossRef](#)]
46. Maryeva, O.; Abolmasov, P. Modelling the optical spectrum of Romano’s star. *Mon. Not. R. Astron. Soc.* **2012**, *419*, 1455–1464. [[CrossRef](#)]
47. Clark, J.S.; Castro, N.; Garcia, M.; Herrero, A.; Najarro, F.; Negueruela, I.; Ritchie, B.W.; Smith, K.T. On the nature of candidate luminous blue variables in M 33. *Astron. Astrophys.* **2012**, *541*, A146. [[CrossRef](#)]
48. Smith, L.J.; Crowther, P.A.; Prinja, R.K. A study of the luminous blue variable candidate He 3-519 and its surrounding nebula. *Astron. Astrophys.* **1994**, *281*, 833–854.
49. Wolf, B. Empirical amplitude-luminosity relation of S Doradus variables and extragalactic distances. *Astron. Astrophys.* **1989**, *217*, 87–91.
50. Clark, J.S.; Larionov, V.M.; Arkharov, A. On the population of galactic Luminous Blue Variables. *Astron. Astrophys.* **2005**, *435*, 239–246. [[CrossRef](#)]
51. Ekström, S.; Georgy, C.; Eggenberger, P.; Meynet, G.; Mowlavi, N.; Wyttenbach, A.; Granada, A.; Decressin, T.; Hirschi, R.; Frischknecht, U.; et al. Grids of stellar models with rotation. I. Models from 0.8 to 120 M $_{\odot}$ at solar metallicity ($Z = 0.014$). *Astron. Astrophys.* **2012**, *537*, A146. [[CrossRef](#)]
52. Hainich, R.; Rühling, U.; Todt, H.; Oskinova, L.M.; Liermann, A.; Gräfener, G.; Foellmi, C.; Schnurr, O.; Hamann, W.R. The Wolf-Rayet stars in the Large Magellanic Cloud. A comprehensive analysis of the WN class. *Astron. Astrophys.* **2014**, *565*, A27. [[CrossRef](#)]
53. Najarro, F. Spectroscopy of P Cygni. In *P Cygni 2000: 400 Years of Progress*; Astronomical Society of the Pacific Conference Series; de Groot, M., Sterken, C., Eds.; The Astronomical Society of the Pacific: San Francisco, CA, USA, 2001; Volume 233, p. 133.
54. Groh, J.H.; Daminieli, A.; Hillier, D.J.; Barbá, R.; Fernández-Lajús, E.; Gamen, R.C.; Moisés, A.P.; Solivella, G.; Teodoro, M. Bona Fide, Strong-Variable Galactic Luminous Blue Variable Stars are Fast Rotators: Detection of a High Rotational Velocity in HR Carinae. *Astrophys. J. Lett.* **2009**, *705*, L25–L30. [[CrossRef](#)]
55. Ferland, G.J.; Korista, K.T.; Verner, D.A.; Ferguson, J.W.; Kingdon, J.B.; Verner, E.M. CLOUDY 90: Numerical Simulation of Plasmas and Their Spectra. *Publ. ASP* **1998**, *110*, 761–778. [[CrossRef](#)]

56. Ferland, G.J.; Chatzikos, M.; Guzmán, F.; Lykins, M.L.; van Hoof, P.A.M.; Williams, R.J.R.; Abel, N.P.; Badnell, N.R.; Keenan, F.P.; Porter, R.L.; Stancil, P.C. The 2017 Release Cloudy. *Revista Mexicana de Astronomía y Astrofísica* **2017**, *53*, 385–438.
57. De Koter, A.; Lamers, H.J.G.L.M.; Schmutz, W. Variability of luminous blue variables. II. Parameter study of the typical LBV variations. *Astron. Astrophys.* **1996**, *306*, 501.
58. Lamers, H.J.G.L.M. Observations and Interpretation of Luminous Blue Variables. In *International Astronomical Union Colloquium*; Astronomical Society of the Pacific Conference Series; Stobie, R.S., Whitelock, P.A., Eds.; Cambridge University Press: Cambridge, UK, 1995; Volume 83, p. 176.
59. Guzik, J.A.; Lovekin, C.C. Pulsations and Hydrodynamics of Luminous Blue Variable Stars. *Astron. Rev.* **2012**, *7*, 13–47. [[CrossRef](#)]
60. Moffat, A.F.J. Wolf-Rayet Stars in the Magellanic Clouds. VII. Spectroscopic Binary Search among the WNL Stars and the WN6/7–WN8/9 Dichotomy. *Astrophys. J.* **1989**, *347*, 373. [[CrossRef](#)]
61. Sterken, C.; van Genderen, A.M.; Plummer, A.; Jones, A.F. Wra 751, a luminous blue variable developing an S Doradus cycle. *Astron. Astrophys.* **2008**, *484*, 463–467. [[CrossRef](#)]
62. Gvaramadze, V.V.; Kniazev, A.Y.; Maryeva, O.V.; Berdnikov, L.N. Optical spectroscopy of the blue supergiant Sk–69° 279 and its circumstellar shell with SALT. *Mon. Not. R. Astron. Soc.* **2018**, *474*, 1412–1425. [[CrossRef](#)]
63. van Genderen, A.M. S Doradus variables in the Galaxy and the Magellanic Clouds. *Astron. Astrophys.* **2001**, *366*, 508–531. [[CrossRef](#)]
64. Toalá, J.A.; Guerrero, M.A.; Ramos-Larios, G.; Guzmán, V. WISE morphological study of Wolf-Rayet nebulae. *Astron. Astrophys.* **2015**, *578*, A66. [[CrossRef](#)]
65. Davidson, K.; Humphreys, R.M.; Hajian, A.; Terzian, Y. He 3-519—A peculiar post-LBV, pre-WN star? *Astrophys. J.* **1993**, *411*, 336–341. [[CrossRef](#)]
66. Foellmi, C.; Koenigsberger, G.; Georgiev, L.; Toledano, O.; Marchenko, S.V.; Massey, P.; Dall, T.H.; Moffat, A.F.J.; Morrell, N.; Corcoran, M.; et al. New insights into the nature of the SMC WR/LBV binary HD 5980. *Rev. Mex.* **2008**, *44*, 3–27.
67. Koenigsberger, G.; Morrell, N.; Hillier, D.J.; Gamen, R.; Schneider, F.R.N.; González-Jiménez, N.; Langer, N.; Barbá, R. The HD 5980 Multiple System: Masses and Evolutionary Status. *Astron. J.* **2014**, *148*, 62. [[CrossRef](#)]



© 2019 by the authors. Licensee MDPI, Basel, Switzerland. This article is an open access article distributed under the terms and conditions of the Creative Commons Attribution (CC BY) license (<http://creativecommons.org/licenses/by/4.0/>).